

# A numerical evaluation of chamber methodologies used in measuring the $\delta^{13}\text{C}$ of soil respiration

Nick Nickerson\* and Dave Risk

Department of Earth Sciences, St. Francis Xavier University, P.O. Box 5000, Antigonish, Nova Scotia, Canada, B2G 2W5

Received 6 January 2009; Revised 26 June 2009; Accepted 4 July 2009

Measurement of the  $\delta^{13}\text{C}$  value of soil-respired  $\text{CO}_2$  ( $\delta_r$ ) has become a commonplace method through which ecosystem function and C dynamics can be better understood. Despite its proven utility there is currently no consensus on the most robust method with which to measure  $\delta_r$ . Static and dynamic chamber systems are both commonly used for this purpose; however, the literature on these methods provides evidence suggesting that measurements of  $\delta_r$  made with these chamber systems are neither repeatable (self-consistent) nor comparable across methodologies. Here we use a three-dimensional (3-D) numerical soil-atmosphere-chamber model to test these chamber systems in a 'surrogate reality'. Our simulations show that each chamber methodology is inherently biased and that no chamber methodology can accurately predict the true  $\delta_r$  signature under field conditions. If researchers intend to use  $\delta_r$  to study *in situ* ecosystem processes, the issues with these chamber systems need to be corrected either by using diffusive theory or by designing a new, unbiased  $\delta_r$  measurement system. Copyright © 2009 John Wiley & Sons, Ltd.

Measurement of the  $\delta^{13}\text{C}$  value of soil respired  $\text{CO}_2$  ( $\delta_r$ ) has become a commonplace method through which ecosystem function and C dynamics can be better understood. Despite its obvious utility there is currently no consensus on the most robust static or dynamic chamber method with which to measure  $\delta_r$ , nor has any consistent approach for analysis of these data emerged.

Non-steady-state static chambers are currently the most commonly used method to determine  $\delta_r$ , possibly because of their affordability and ease of use.<sup>1–7</sup> In their simplest form, these chambers consist of a 'cap' which is placed on the soil surface to collect soil  $\delta^{13}\text{C}$ - $\text{CO}_2$  emissions. To determine  $\delta_r$ , these static chambers are sampled several times over a given deployment period and the data are used to construct a Keeling plot. The Keeling plot, a graphical representation of Keeling's two end-member mixing model (see Ohlsson *et al.*<sup>1</sup> or Pataki *et al.*<sup>8</sup> for a more detailed description of the Keeling approach), is used along side linear regression techniques to provide estimates of  $\delta_r$ . Field and laboratory trials have shown that the static chamber-Keeling plot method (hereafter referred to as the Static method) appears to be reliable and linear over a wide range of scenarios; however, some concern about the linearity of the method at high  $\text{CO}_2$  concentration has been raised.<sup>1,9,10</sup> In addition to possible methodological issues associated with the Static approach, several studies<sup>8,11</sup> have also shown that statistical error and natural variability can bias Keeling plot estimates of  $\delta_r$  significantly.

As an alternative to the Static approach, some researchers have used a Static chamber modification in which the chamber is purged first to help eliminate existing atmospheric  $\delta^{13}\text{C}$  fingerprints (*viz.* Buchmann and Ehleringer<sup>3</sup>). For this purged chamber method, the value of  $\delta_r$  has been derived either using the Keeling plot approach<sup>1</sup> or simply by taking a single sample of chamber  $\text{CO}_2$  after sufficient chamber concentration buildup. The assumption of this single sample method is that, because the chamber is initially purged, all (or most) of the chamber  $\text{CO}_2$  must be derived from efflux and thus the chamber's isotopic signature must be equal to  $\delta_r$ . The single sample purged chamber method (herein referred to as Purged-S) has been used in several studies<sup>3,12</sup> with seemingly good results; however, the method has never been rigorously tested to ensure that it measures  $\delta_r$ . For the Keeling plot-purged chamber method (abbreviated Purged-K for the remainder of the paper), careful examination of the method by Ohlsson *et al.*<sup>1</sup> revealed that it probably does not measure  $\delta_r$ ; rather, it is hypothesized to measure some fractionated value because of the disturbance to the soil  $\text{CO}_2$  diffusive regime caused by the purging procedure.

More recently, Mora and Raich<sup>13</sup> have suggested the method of simply allowing a Static chamber to remain on the soil surface for long time periods so that  $\text{CO}_2$  concentrations within the chamber headspace reach a natural, soil efflux-driven equilibrium. After equilibrium is attained the authors hypothesize that the  $\delta^{13}\text{C}$  in the chamber should reflect the value of  $\delta_r$ . When this method (referred to as the Mora chamber for the remainder of the paper) was tested by Mora and Raich<sup>13</sup> the authors concluded that the chamber methodology accurately reflected the value of  $\delta_r$  at their field site. However, this result is in direct conflict with the recent findings of Kayler *et al.*<sup>2</sup> who found that the Mora

\*Correspondence to: N. Nickerson, Department of Earth Sciences, St. Francis Xavier University, P.O. Box 5000, Antigonish, Nova Scotia, Canada, B2G 2W5.  
E-mail: nnickers@stfx.ca  
Contract/grant sponsor: Natural Sciences and Engineering Research Council.

method better reflected the  $\delta^{13}\text{C}$  value of soil  $\text{CO}_2$  at the soil collar insertion depth.

Steady-state chamber designs may be more appropriate and less error prone than the aforementioned static chamber approaches for gaining estimates of  $\delta_r$  in diffusive environments. These chambers are typically more complex, but should offer improved and more accurate measurements of  $\delta_r$  by eliminating or controlling disturbance to the natural  $\text{CO}_2$  and  $\delta^{13}\text{C}$  gradients. One steady-state chamber design, developed by Subke *et al.*<sup>14</sup> and tested by Bertolini *et al.*<sup>15</sup> and similar to the design described by Midwood *et al.*,<sup>16</sup> maintains the chamber headspace concentration at ambient atmospheric concentration using a  $\text{CO}_2$  sorbent (i.e. soda lime) and a variable speed pump. This allows the natural soil-atmosphere  $\text{CO}_2$  gradient to be held near its steady-state condition, theoretically eliminating biases associated with non-steady-state diffusion processes.<sup>14,17,18</sup> However, there is conflicting evidence as to what is actually being measured by these steady-state chamber methodologies. Experimental data presented in Bertolini *et al.*<sup>15</sup> showed that the chamber design described by Subke *et al.*<sup>14</sup> (hereafter referred to as the Bertolini chamber) yielded  $\delta^{13}\text{C}$  values that were characteristic of soil  $\text{CO}_2$  rather than of soil-respired  $\text{CO}_2$ . The authors hypothesized that this result may be due to the disturbance of the natural  $^{13}\text{CO}_2$  gradient and subsequent lateral diffusion effects that would result from this disturbance. However, tests performed using the chamber developed by Midwood *et al.*,<sup>16</sup> which is based on the same principles as the design of Subke *et al.*,<sup>14</sup> showed that the method measured the true  $\delta^{13}\text{C}$  value of soil-respired  $\text{CO}_2$  rather than that of soil  $\text{CO}_2$ .

Considering the large amount of conflicting evidence and uncertainty in both non-steady-state and steady-state chamber methodologies, it is clear that a broader theoretical understanding of these methodologies is needed. In this paper we use a previously validated<sup>10</sup> three-dimensional (3-D) numerical soil-atmosphere model designed to simulate both in-soil and emitted  $\delta^{13}\text{C}$  signatures. This model environment provides us with a surrogate reality to theoretically test the robustness of these non-steady-state and steady-state sampling methodologies. First we explore the possible sources for the conflicting experimental evidence and show that non-steady-state lateral diffusion is an important consideration for interpreting chamber measurements of  $\delta_r$ . Next we evaluate the performance and the reliability of  $\delta_r$  estimates made using each chamber method over a range of production and soil diffusivity scenarios, providing estimates of inter- and intra-methodological error. Finally, we make recommendations as to the methodologies and analytical techniques that most accurately reflect  $\delta_r$  and outline the need for further research.

## EXPERIMENTAL

### Soil-atmosphere model

The numerical soil-atmosphere isotopologue model<sup>9,10,18</sup> simulates the 3-D transport of gases through the soil column and into the overlying atmosphere. The model consists of a constant concentration atmospheric boundary layer and a soil cylinder of length  $L$  (m) and radius  $R$  (m) that includes

solid matter, air-filled and water-filled pore spaces (for all simulations presented in this paper,  $L=0.25$  m and  $R=0.125$  m). The soil column is divided into 10 vertical and 5 radial soil layers of size  $L/10$  and  $R/5$ , respectively, each having its own layer specific total, air-filled and water-filled porosity, effective diffusivity value and  $\text{CO}_2$  production rate. Exchange of  $\text{CO}_2$  between model layers is controlled by Fick's law:

$$F_{ij} = -D_{ij} \frac{\Delta C_{ij}}{\Delta(z, r)_{ij}} \quad (1)$$

where  $D_{ij}$  is the effective diffusion coefficient ( $\text{m}^2 \text{s}^{-1}$ ) between the two soil layers in question (layer  $i$  and layer  $j$ ),  $\Delta C_{ij}$  is the difference in layer  $\text{CO}_2$  concentrations ( $\mu\text{mol m}^{-3}$ ) and  $\Delta(z, r)_{ij}$  is the difference in the positions (m) of the layers.

After each time step the new  $\text{CO}_2$  concentration ( $C_i(z, r, t)$ ,  $\mu\text{mol m}^{-3}$ ) in each layer is calculated according to:<sup>19</sup>

$$C_i(z, r, t) = C_i(z, r, t - 1) + \left[ \frac{F(z - 1) - F(z) + F(r - 1) + F(r + 1) + \gamma}{\theta V_l} \right] \quad (2)$$

where  $C_i(z, r, t - 1)$  is the layer concentration at the previous time step,  $\theta$  is the soil air-filled pore space ( $v/v$ ),  $F(z - 1)$  is the flux from the layer below,  $F(z)$  is the flux leaving the layer,  $F(r - 1)$  and  $F(r + 1)$  are the fluxes coming from laterally adjacent soil layers,  $\gamma$  is the biological production rate of  $\text{CO}_2$  ( $\mu\text{mol m}^{-3} \text{s}^{-1}$ ), and  $V_l$  is the volume of the layer ( $\text{m}^3$ ). In the event that  $z=L$  or  $r=R$ , Eqn. (2) is modified to exclude the terms  $F(z - 1)$  and  $F(r + 1)$  in accordance with there being no flux boundary conditions placed at these positions.

Soil effective diffusivity is calculated using the modified Millington-Quirk relationship, which relates pore space and diffusivity:<sup>20</sup>

$$D_e = \left[ \frac{\phi^{10/3} D_{fw} + \theta^{10/3} D_{fa}}{H} \right] \cdot \theta_T^{-2} \quad (3)$$

where  $\phi$  is the water-filled pore space,  $\theta$  is the air-filled pore space,  $\theta_T$  is the total pore space,  $D_{fw}$  and  $D_{fa}$  are the diffusion coefficients of  $\text{CO}_2$  in free water and free air, respectively, and  $H$  is a dimensionless form of Henry's solubility constant for  $\text{CO}_2$  in water ( $H=0.8317$ ).

For the purposes of these simulations, production ( $\gamma$ ) of  $\text{CO}_2$  is partitioned equally over all vertical soil layers, with no radial variation. To minimize the model run time, the model is initialized using the analytical solution for a steady-state system under the same assumptions. The initial  $\text{CO}_2$  concentration at each depth is calculated as follows:<sup>21</sup>

$$C(z) = \frac{\gamma}{LD_e} \left( Lz - \frac{z^2}{2} \right) + C_{\text{atm}} \quad (4)$$

where  $C(z)$  is the concentration ( $\mu\text{mol m}^{-3}$ ) at depth  $z$  (m),  $L$  (m) is the depth of the soil column and  $C_{\text{atm}}$  is the concentration of  $\text{CO}_2$  in the atmospheric layer ( $\mu\text{mol m}^{-3}$ ).

To model the isotopic composition of soil  $\text{CO}_2$  and  $\text{CO}_2$  efflux each carbon isotopologue of  $\text{CO}_2$  ( $^{12}\text{CO}_2$  and  $^{13}\text{CO}_2$ ) is treated separately with an isotopologue specific atmospheric concentration, production and diffusion rate (see Nickerson and Risk<sup>18</sup> for more detail). This allows two instances of the model to be run and the resulting concentrations and fluxes

of each isotopic species can then be used to calculate the  $\delta^{13}\text{C}$  signatures of the soil  $\text{CO}_2$  and surface flux at each time step.

The model was programmed in Perl and all model runs were performed under the Macintosh OS X operating system. All solutions were found by Euler integration with a time step of  $10^{-3}$  s.

### Chamber models

Each numerical chamber model is based on a physical chamber embodiment that has been previously used in field or laboratory studies. The chamber, when deployed, occupies the first two (starting from the centre) radial layers of the soil-atmosphere model. The chamber is considered to be perfectly mixed, regardless of size, and is allowed to interact with the soil diffusively via Fick's Law (Eqn. (1)). Each chamber design fills with  $\text{CO}_2$  according to different numerical conditions, described below.

The numerical model for the Static chamber was based on the chamber of Ekblad and Högborg.<sup>4</sup> The chamber is cylindrical and has a diameter of 10 cm and height of 5 cm. When deployed on the soil surface the time evolution of chamber  $\text{CO}_2$  concentration can be described by simple mass balance as:

$$C_c(t) = C_c(t-1) + \frac{F_s(t)A_c}{V_c} \quad (5)$$

where  $C_c(t-1)$  is the chamber  $\text{CO}_2$  concentration at the previous time step,  $V_c$  is the chamber volume,  $F_s(t)$  is the surface flux from soil to chamber during the current time step and  $A_c$  is the surface area of the chamber.

The Purged chamber is an extension of the design of Ekblad and Högborg<sup>4</sup> with the same geometry, similar to the chamber used in Ohlsson *et al.*<sup>1</sup> Similarly, the filling of the chamber is described by Eqn. (5); however, to mimic the purging process, the initial chamber concentration is assumed to be instantaneously reduced to 5% of atmospheric at model time zero while maintaining the ambient atmospheric  $\delta^{13}\text{C}$  signature.

The numerical model for the Mora chamber is based on the chamber described in Mora and Raich.<sup>13</sup> This design consists simply of a Static chamber that is left on the soil for long periods of time to ensure full diffusive equilibration with surface efflux. The simulated chamber geometry is cylindrical with a diameter of 10 cm and height of 5 cm. The filling of the chamber is described by Eqn. (5).

Finally, we based our numerical Bertolini chamber model after the chamber design of Subke *et al.*<sup>14</sup> The modeled chamber geometry is cylindrical, with a diameter of 10 cm and a height of 10 cm. The chamber  $\text{CO}_2$  concentration is monitored using a logic switch (if/else) to ensure that the steady-state (atmospheric) concentration is maintained within the chamber headspace during the simulation. When the chamber concentration differs from the ambient atmospheric concentration the model alters the pump speed of air passing over a perfectly absorbent soda lime column, thereby increasing or decreasing the  $\text{CO}_2$  concentration back to the ambient level. At each model time step, filling of the Bertolini chamber with soil  $\text{CO}_2$  is described by Eqn. (5). Loss of  $\text{CO}_2$  from the chamber headspace due to absorption by soda lime

is calculated as:

$$C_{\text{loss}}(t) = \nu \varepsilon C_c(t-1) \quad (6)$$

where  $\nu$  is the pump speed ( $\text{m}^3 \text{s}^{-1}$ ) and  $\varepsilon$  is the soda lime efficiency ( $\varepsilon = 1$ , perfect absorber with no isotopic fractionation). The final chamber concentration at each time step is calculated by subtracting the result of Eqn. (6), the loss due to soda lime, from the result of Eqn. (5), the gain from soil flux.

To mimic field deployments all chamber models include a soil collar of variable length  $\xi$  (m), which prevents diffusion from the edge of the chamber (second radial layer) to the next radial soil layer. To simulate 1-D diffusion scenarios,  $\xi$  is set equal to  $L$ , the total soil column length, which prevents any lateral diffusion of soil gases. Shortening the soil collar depth ( $\xi < L$ ) allows the study of lateral diffusion effects on chamber  $\text{CO}_2$  and  $\delta^{13}\text{C}$  evolution.

### Model validation and simulation conditions

The model function was validated using both steady- and non-steady-state analytical solutions to the diffusion equation<sup>18</sup> and the coupled chamber models were validated using the non-steady-state analytical solution described by Livingston *et al.*<sup>17</sup> Further Static chamber specific experimental validation of the model is provided in Nickerson and Risk.<sup>10</sup>

In this work, the chamber  $\text{CO}_2$  concentrations and  $\delta^{13}\text{C}$  signatures were simulated for a range of soil production rates ( $0.1$  to  $10 \mu\text{mol m}^{-2} \text{s}^{-1}$ ) and diffusivity coefficients ( $0.005$  to  $3.8 \times 10^{-6} \text{m}^2 \text{s}^{-1}$ ). In all simulations the atmospheric  $\text{CO}_2$  concentration and isotopic signature were assumed to be 400 ppm and  $-8\text{‰}$ , respectively. Similarly, the production  $\delta^{13}\text{C}$  signature, or  $\delta_r$ , was assumed to have a fixed value of  $-25\text{‰}$ , a value that is typical of soil respiration at  $C_3$  field sites.<sup>4,13</sup>

For our chamber reliability and comparability scenarios we used common field sampling and analytical methodologies to make our model data more directly comparable with empirical data. For Static chamber simulations a deployment period of 10 min and a sampling interval of 2 min (six measurements in total including  $t = 0$ ) was used in the construction of Keeling plots and ordinary least-squares (OLS) regression was used in the estimation of  $\delta_r$ .<sup>4</sup> For the purged Purged-S and Purged-K chambers, chamber concentrations were initially reduced to 5% of ambient atmospheric concentration.<sup>3</sup> For the Purged-S method chamber the  $\delta^{13}\text{C}$  signature was singly sampled after the chamber reached an internal concentration of 350 ppm.<sup>3</sup> For the Purged-K method, the chamber headspace was sampled using the same protocol as for the Static chamber, and Keeling plots were constructed and analyzed (OLS) using these data.<sup>14</sup>

For the Mora chamber a single  $\delta^{13}\text{C}$  measurement is made after chamber equilibration. Equilibrium is defined by the decrease of the time derivative of both the  $\text{CO}_2$  concentration and the  $\delta^{13}\text{C}$  signature to zero ( $\pm 0.01 \text{ppm CO}_2 \text{s}^{-1} / 0.001\text{‰ s}^{-1}$ ).<sup>18</sup> Finally, for the Bertolini chamber a single  $\delta^{13}\text{C}$  measurement was made after chamber  $\delta^{13}\text{C}$  equilibration (usually within 1–3 h of deployment time, depending on flux rates).<sup>14,15</sup>

## RESULTS AND DISCUSSION

## Static and Mora chambers

Not surprisingly, when the simulations for the Static and Mora chamber were compared they showed identical results due to their similar designs and deployment strategies. Because of this, we have combined these results and will present them in the current section. Shown in Fig. 1 is the simulated 1-D ( $\xi = L$ ;  $\text{CO}_2$  can diffuse only in the z-direction with no lateral movement) time series (24 h) evolution of Static/Mora chamber  $\text{CO}_2$  concentrations and  $\delta^{13}\text{C}$  signatures for model soils with varying production and diffusion rates. For the Mora sampling approach (taking a single sample after the chamber has reached equilibrium) it is clear from Fig. 1 that, even after chamber  $\delta^{13}\text{C}$  signatures have reached a stable value, they are still  $\sim 1\%$  different from the simulated signature of soil production. Comparison of these model results with the results of a simulation in which the chamber conditions could not influence soil conditions (data not shown) shows that this  $\sim 1\%$  discrepancy is the result of chamber-to-soil feedbacks; i.e., the change in the  $\text{CO}_2$  concentration and  $\delta^{13}\text{C}$  signature within the chamber feeding back and changing  $\text{CO}_2$  concentrations and  $\delta^{13}\text{C}$  signatures within the soil below the chamber. These chamber-to-soil feedbacks cause non-steady-state differential diffusion of  $\text{CO}_2$  isotopologues driven by the fact that  $^{12}\text{CO}_2$  diffuses 1.0044 times faster<sup>9</sup> than  $^{13}\text{CO}_2$ . Because these chamber-to-soil feedbacks will always be present in both field and experimental work this result implies that estimates of  $\delta_r$  made using the approach of Mora and Raich<sup>13</sup> are probably inherently biased by this effect. For the Static chamber approach, Keeling plots for 1-D simulations show distinct non-linearities<sup>10</sup> made more evident by their derivatives,

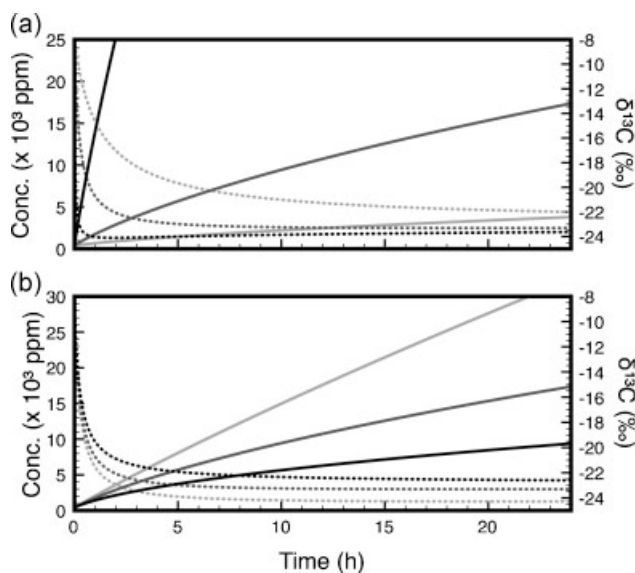


**Figure 1.** Time series evolution for simulated Static chamber  $\text{CO}_2$  concentrations (solid lines) and  $\delta^{13}\text{C}$  signatures (dashed lines). (a) Production rates of  $0.2 \mu\text{mol m}^{-3} \text{s}^{-1}$  (light grey),  $1 \mu\text{mol m}^{-3} \text{s}^{-1}$  (dark grey) and  $10 \mu\text{mol m}^{-3} \text{s}^{-1}$  (black) at a stable diffusivity of  $4.68 \times 10^{-7} \text{m}^2 \text{s}^{-1}$ . (b) Diffusivity rates of  $4.66 \times 10^{-8} \text{m}^2 \text{s}^{-1}$  (light grey),  $4.68 \times 10^{-7} \text{m}^2 \text{s}^{-1}$  (dark grey) and  $1.81 \times 10^{-6} \text{m}^2 \text{s}^{-1}$  (black) at a stable production rate of  $1 \mu\text{mol m}^{-3} \text{s}^{-1}$ .

presented in Fig. 2. These Keeling plot non-linearities are also caused by chamber-to-soil diffusive feedbacks (causing differential diffusion) and violate key assumptions of the Keeling plot approach. This feedback leads to linear regression estimates of  $\delta_r$  that are enriched (range of enrichment  $\sim 0$ – $1.1\%$  for a 40 min chamber deployment, see Nickerson and Risk<sup>10</sup> for more data) compared with the actual  $\delta_r$  signature because of the concave-up curvature of feedback-affected Keeling plots.

When the soil collars were shortened ( $\xi < L$ ;  $\text{CO}_2$  can diffuse in both the z and r directions) simulations showed that lateral effects caused by diffusion of  $\text{CO}_2$  around soil collars becomes an important consideration for both methodologies.<sup>10</sup> Lateral diffusion effects were negligible for all simulated soil collar lengths (range: 2.50–25.0 cm) when the soil diffusivity and air-filled porosity were low and when the chamber deployment time was short. This limited lateral diffusion is a direct effect of the relationship between soil diffusivity, distance and time. When the soil diffusivity is low, chamber-to-soil feedbacks take much longer to occur because the soil  $\text{CO}_2$  profiles are more resistant to change. This increases the time that it takes for chamber-driven soil  $\text{CO}_2$  disturbances to propagate to the bottom of the soil collar and, therefore, increases the time that it takes for lateral diffusion to become a significant portion of the total gas movement. For this reason the time evolution of the chamber concentrations and the  $\delta^{13}\text{C}$  signatures follows a trajectory similar to those simulated in the 1-D case. However, when

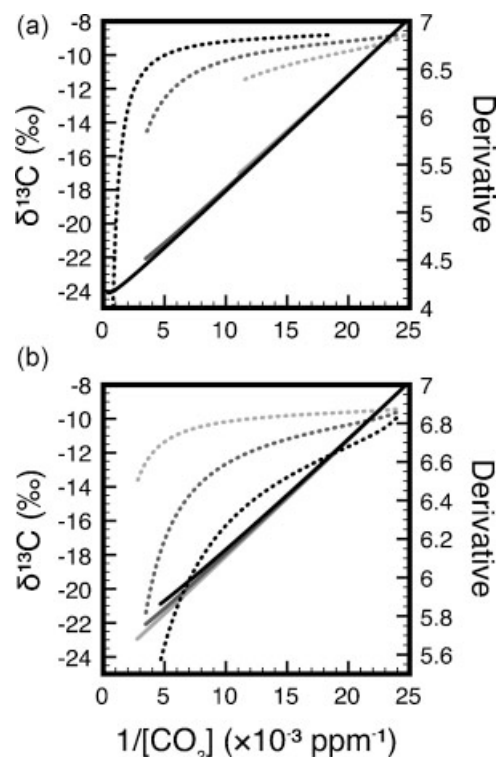


**Figure 2.** Keeling plots for selected simulated Static chamber scenarios (solid lines) and their derivatives (dashed lines). (a) Production rates of  $0.2 \mu\text{mol m}^{-3} \text{s}^{-1}$  (light grey),  $1 \mu\text{mol m}^{-3} \text{s}^{-1}$  (dark grey) and  $10 \mu\text{mol m}^{-3} \text{s}^{-1}$  (black). (b) Diffusivity rates of  $4.66 \times 10^{-8} \text{m}^2 \text{s}^{-1}$  (light grey),  $4.68 \times 10^{-7} \text{m}^2 \text{s}^{-1}$  (dark grey) and  $1.81 \times 10^{-6} \text{m}^2 \text{s}^{-1}$  (black).

the modeled soil diffusivity increased, chamber-to-soil feedback rates also increased, as did the effect of the lateral diffusion of soil gases around the collar, with the greatest deviations from the 1-D simulations occurring when the soil collar was short (2.5 cm) and soil diffusivities were high. This lateral diffusion resulted in decreased (compared with the 1-D case) chamber CO<sub>2</sub> concentrations and increased (more enriched)  $\delta^{13}\text{C}$  values within the chamber head space, shown in Fig. 3.

In some cases the  $\delta^{13}\text{C}$  signatures in the chamber headspace become transiently lighter (more negative) than their equilibrium value before asymptotically returning to equilibrium after sufficient time had elapsed (light and dark grey lines in Fig. 3). Further analysis of these data showed that where lateral diffusion is present, Static and Mora chambers appear to initially tend toward equilibrium with soil-respired  $\delta^{13}\text{C}\text{-CO}_2$  but once the lateral gas flux becomes significant compared with the vertical gas flux, the chambers begin to equilibrate with soil CO<sub>2</sub> at the base of the soil collar (see Fig. 3). In concurrence with the results presented in Risk and Kellman<sup>9</sup> increases in simulated production rate caused increases in the magnitude of the transient dip in  $\delta^{13}\text{C}\text{-CO}_2$  signature, given the same diffusivity, and increases in soil diffusivity caused the dip to occur sooner given the same production rate (not shown here but discussed in Risk and Kellman<sup>9</sup>).

Finally, Keeling plots constructed for 3-D diffusion simulations showed stronger concave-up curvature than their 1-D counterparts.<sup>10</sup> This increased curvature is due to a combination of chamber-to-soil feedback mechanisms, as in the 1-D case, and lateral diffusion effects that only occur when diffusion is allowed to occur in 3-D. Previous analysis of these lateral diffusion Keeling plots showed potential Keeling intercept errors of up to 4‰ in high-diffusivity low-production scenarios where chamber-to-soil feedbacks are greatest.<sup>10</sup>

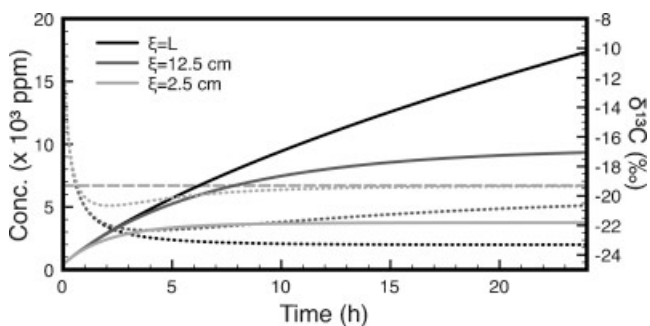


**Figure 3.** Time series evolution for simulated Static chamber CO<sub>2</sub> concentrations (solid lines) and  $\delta^{13}\text{C}$  signatures (dashed lines) for a production rate of  $0.2 \mu\text{mol m}^{-3} \text{s}^{-1}$ . Black lines show the 1-D ( $\xi = L$ ) time evolution whereas dark and light grey lines show the time evolution with soil collar depths ( $\xi$ ) of 12.5 and 2.5 cm, respectively. Note both the dip behaviour of the  $\delta^{13}\text{C}$  curve and the final equilibration of the chamber  $\delta^{13}\text{C}$  signatures with soil  $\delta^{13}\text{C}$  signatures at the depth of the soil collar (shown for  $\xi = 2.5$  cm, short dashed line represents chamber signature and long dashed line shows soil  $\delta^{13}\text{C}$  signature at the base of the collar).

This simulated non-linear behaviour in the Keeling plot was recently experimentally noted by Risk and Kellman<sup>9</sup> who showed that it was probably an effect of the differential diffusion of CO<sub>2</sub> isotopologues. While no deviations from linearity have been seen in previous field studies that have used the Static chamber approach (i.e. Ohlsson *et al.*<sup>1</sup> and Ekblad and Högberg<sup>4</sup>) it is plausible that the predicted non-linear behaviour of the Keeling plot is not distinguishable because of error due to sampling methodologies (i.e. sample extraction and analysis errors) or variability created by non-steady-state diffusive processes.<sup>17,22</sup>

The Mora chamber was found to equilibrate with a value close to  $\delta_r$  under 1-D diffusion, as was expected by Mora and Raich,<sup>13</sup> however, when lateral diffusion around soil collars was taken into account, the method was found to equilibrate with soil  $\delta^{13}\text{C}\text{-CO}_2$  rather than with  $\delta_r$  as was observed in Kayler *et al.*<sup>2</sup> Unfortunately, this type of equilibrium in the Mora chamber means that a steady-state diffusion model<sup>7</sup> must be applied if the source signature is to be known, leading to potentially large error because of uncertainty in soil parameter estimates and possible dynamic fractionation effects.<sup>18</sup> While this model result seems to contrast with the experimental results of Mora and Raich<sup>13</sup> which showed equilibration with  $\delta_r$ , we argue that the chamber used by the authors probably equilibrated with CO<sub>2</sub> deep in the soil profile and that the isotopic signature of respiration in these ecosystems is probably at least 4.4‰ depleted<sup>7</sup> from their measured values.

### Purged chamber

Similar to the 1-D Static case, simulated (1-D) Purged chambers were found to equilibrate with an isotopic value close ( $\sim 1\%$  offset) to  $\delta_r$  after sufficient deployment time (Fig. 4). Because of the reduced atmospheric CO<sub>2</sub> fingerprint

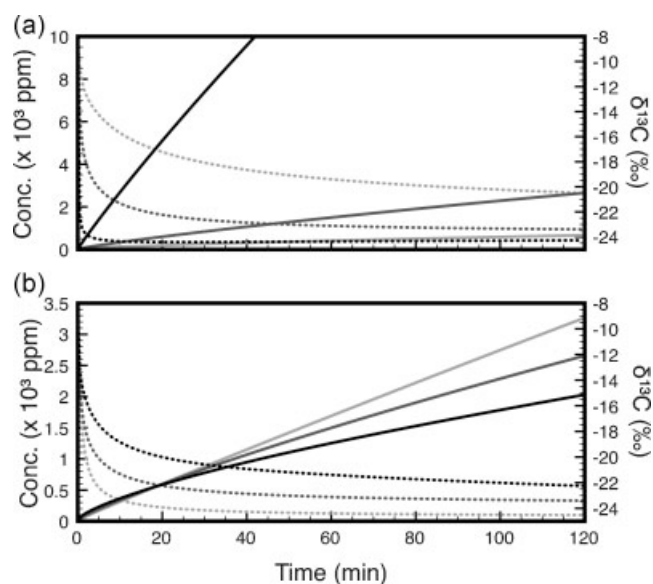


**Figure 4.** Time series evolution for simulated Purged chamber CO<sub>2</sub> concentrations (solid lines) and  $\delta^{13}\text{C}$  signatures (dashed lines). (a) Production rates of  $0.2 \mu\text{mol m}^{-3} \text{s}^{-1}$  (light grey),  $1 \mu\text{mol m}^{-3} \text{s}^{-1}$  (dark grey) and  $10 \mu\text{mol m}^{-3} \text{s}^{-1}$  (black). (b) Diffusivity rates of  $4.66 \times 10^{-8} \text{m}^2 \text{s}^{-1}$  (light grey),  $4.68 \times 10^{-7} \text{m}^2 \text{s}^{-1}$  (dark grey) and  $1.81 \times 10^{-6} \text{m}^2 \text{s}^{-1}$  (black).

within the chamber the required deployment time before equilibrium was shorter for Purged chambers than for Static chambers. For the Purged-S (single sample) method, Fig. 4 makes it abundantly clear that although purging reduces the initial atmospheric contribution in the chamber significantly, a single measured value of chamber  $\delta^{13}\text{C}$  is unlikely to reflect  $\delta_r$ , even after full equilibrium has been attained.

Keeling plots constructed for Purged chambers (Fig. 5) showed considerable non-linearity, especially considering that Keeling plots for the 1-D Static simulations showed only slight concave-up curvature. This extreme non-linearity is a direct result of the initial drop in chamber  $\text{CO}_2$  concentration caused by the purging process. Reduction of the chamber concentration causes a perturbation to the steady-state  $\text{CO}_2$  flux, which in turn allows isotopically heavy (because of atmospheric invasion)  $\text{CO}_2$  from the soil surface layers to diffuse into the chamber headspace. This effect is transient and after the chamber  $\text{CO}_2$  concentrations have reached or exceeded the ambient atmospheric  $\text{CO}_2$  concentration the Keeling plot data curve to become similar (but not the same as, because of the initial perturbations) to Keeling plot data collected by Static chambers (qualitatively illustrated in Fig. 6(a)). In all 1-D cases Keeling plot intercepts estimated using Purged chamber data were significantly more positive than the actual value of  $\delta_r$  (range of  $\sim 0$ – $15\%$  over all diffusivities and production rates), with the largest deviations occurring when the soil production is low and the soil diffusivity is high.

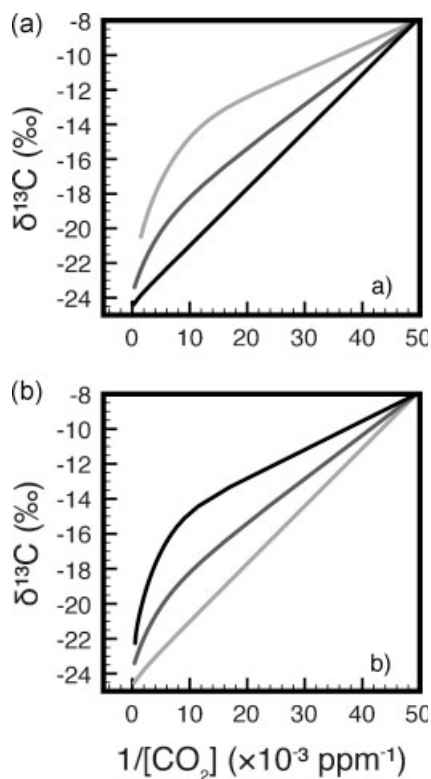


**Figure 5.** Keeling plots for selected simulated Purged-K scenarios. (a) Production rates of  $0.2 \mu\text{mol m}^{-3} \text{s}^{-1}$  (light grey),  $1 \mu\text{mol m}^{-3} \text{s}^{-1}$  (dark grey) and  $10 \mu\text{mol m}^{-3} \text{s}^{-1}$  (black). (b) Diffusivity rates of  $4.66 \times 10^{-8} \text{ m}^2 \text{ s}^{-1}$  (light grey),  $4.66 \times 10^{-7} \text{ m}^2 \text{ s}^{-1}$  (dark grey) and  $1.81 \times 10^{-6} \text{ m}^2 \text{ s}^{-1}$  (black).

We also considered the effect of lateral diffusion on the Purged chambers. Simulations show that, like the Static chamber, the Purged chamber will equilibrate eventually with soil  $\text{CO}_2$  isotopic signatures at the base of the soil collar rather than with the signature of soil flux because of lateral diffusion. The Purged time series data also shows the dip behaviour noted in the Static case but this dip was found to occur sooner and to have a greater magnitude in Purged chambers because of the reduced initial atmospheric concentration. Keeling plots constructed for the lateral diffusion case are, again, non-linear and Keeling intercepts are more enriched than  $\delta_r$  (range of  $\sim 0$ – $15\%$  over all diffusivities and production rates). Single samples of chamber  $\delta^{13}\text{C}$  signatures under lateral diffusion are, in general, more enriched than the expected value of  $\delta_r$  with the enrichment magnitude depending on the soil  $\delta^{13}\text{C}$  at the base of the collar.

Interestingly, the behaviour predicted by our Purged chamber model has also been seen experimentally by Ohlsson *et al.*<sup>1</sup> (shown for comparison in Fig. 6(b)), where the hypothesis that disturbance to the soil  $\text{CO}_2$  gradient causes a non-linear effect in the Keeling plot was first presented.

### Bertolini chamber

Simulated characteristic 1-D ( $\xi=L$ ) time evolutions for chamber  $\delta^{13}\text{C}$  signatures for the Bertolini chamber are shown for varying production rates in Fig. 7(a) and varying diffusivity coefficients in Fig. 7(b). In all 1-D cases the chamber  $\delta^{13}\text{C}$  signatures were found to asymptotically approach the isotopic signature of biological respiration,  $\delta_r$ , given sufficient time. The speed of chamber  $\delta^{13}\text{C}$  equilibration depended mainly on production rate, with increased production leading to quicker equilibration of the chamber  $\delta^{13}\text{C}$  signature but the equilibration speed also had a weak inverse dependence on diffusivity where low diffusivity soils equilibrated marginally faster than high diffusivity soils.

When soil collar lengths were shortened ( $\xi < L$ ) chamber  $\delta^{13}\text{C}$  signatures were found to asymptotically approach more enriched  $\delta^{13}\text{C}$  values rather than  $\delta_r$ . The enrichment magnitude of the measured value from  $\delta_r$  depended on atmospheric and biological production  $\delta^{13}\text{C}$  values, soil diffusivity, biological production rate and collar depth. Further examination of soil  $\delta^{13}\text{C}$  gradients for all simulations showed that the enriched value measured by the Bertolini method is  $\sim 4.4\%$  depleted from the soil air signature at the base of the soil collar (Table 1). This result implies that lateral diffusion of gases around the soil collar causes equilibration of the chamber air with soil air at the base of the collar, as was the case in the Static, Mora and Purged chamber simulations. However, unlike the other chamber designs, the use of a sorbent to maintain ambient atmospheric concentration in the chamber headspace means that  $\text{CO}_2$  continues to diffuse from the soil to chamber rather than diffusing laterally around the chamber because of the maintained ambient bulk  $\text{CO}_2$  gradients. Because of the continual diffusion of  $\text{CO}_2$  into the chamber head space, the diffusive fractionation of  $4.4\%$  must be accounted for.

Under lateral diffusion scenarios the Bertolini method does not measure  $\delta_r$ ; rather, the measured value is the soil

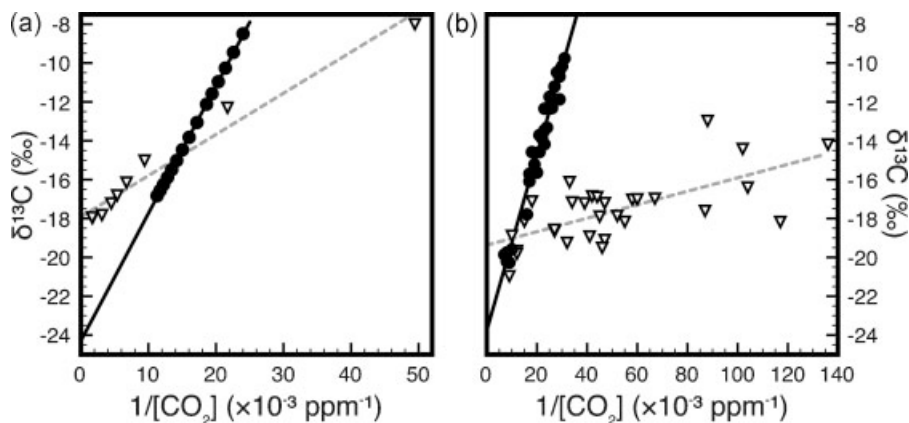


**Figure 6.** Conceptual comparison between model generated (a) Keeling plots for the Static and Purged chamber methodologies and Keeling plots constructed based on experimental data collected by Ohlsson *et al.*<sup>1</sup> (b). Solid circles show the isotopic and concentration data collected using a Static chamber without purging with the black lines showing the best linear fit to the data. Open triangle show the isotopic and concentration data collected using a purged Static chamber with the grey dashed lines showing the best linear fit to these data. It should be noted that no attempt was made here to match experimental and model data.

δ<sup>13</sup>C – 4.4‰ to account for diffusive fractionation. Despite this, if soil collars are deep enough the methodology may reproduce a value close to δ<sub>r</sub> because the method measures a value that is –4.4‰ fractionated from the soil value, which at sufficient depth should be equal to δ<sub>r</sub> + 4.4‰.<sup>7,21,23</sup> Unfortunately, the use of deep soil collars may shear shallow plant roots leading to unwanted disturbance of natural CO<sub>2</sub> production regimes in the measurement area. In addition, the

soil collar depth required to accurately estimate δ<sub>r</sub> depends on the soil diffusivity and the production rate, and, therefore, a fixed length collar will not work in all instances even at the same site. Bertolini *et al.*<sup>15</sup> suggest using their chamber together with a steady-state diffusion model<sup>7</sup> as a way to estimate δ<sub>r</sub> values. While this approach may be possible in some situations, it is important to note that uncertainty in hard to measure parameters such as soil diffusivity and CO<sub>2</sub> production profiles can lead to significant error in estimates of δ<sub>r</sub>. Furthermore, dynamic fractionation effects caused by time varying soil processes<sup>18,22</sup> can impart additional bias on steady-state calculations of δ<sub>r</sub>.

We would also like to note the potential for bias in these measurements due to sorbent fractionation.<sup>24</sup> In the case that the CO<sub>2</sub> sorption efficiency is different for <sup>12</sup>CO<sub>2</sub> and <sup>13</sup>CO<sub>2</sub> the use of the continuous flow sorbent system could skew results significantly by incorporating this measurement-specific fractionation into estimates of δ<sub>r</sub>. This potential problem can be circumvented by using an alternative source of CO<sub>2</sub>-free air, such as a nitrogen/oxygen mixture,<sup>16</sup> to maintain the ambient CO<sub>2</sub> concentration.

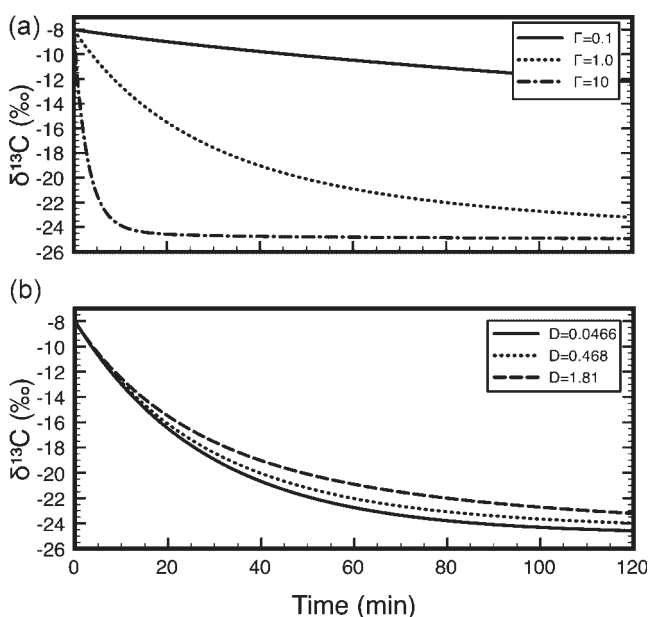


**Figure 7.** (a) Time evolution (1-D transport) of Bertolini chamber δ<sup>13</sup>C signatures for total soil production rates ranging from 0.1 to 10 μmol m<sup>-3</sup> s<sup>-1</sup>. (b) Time evolution (1-D transport) of Bertolini chamber δ<sup>13</sup>C signatures for soil diffusivity rates ranging from 4.66 × 10<sup>-8</sup> m<sup>2</sup> s<sup>-1</sup> to 1.81 × 10<sup>-6</sup> m<sup>2</sup> s<sup>-1</sup>.

**Table 1.** Model air-filled (θ<sub>a</sub>) pore space, CO<sub>2</sub> production rate (γ), measured equilibrium (10 h) Bertolini chamber δ<sup>13</sup>C value, steady-state soil air δ<sup>13</sup>C at the bottom of the soil collar (10 cm deep) and chamber δ<sup>13</sup>C minus soil air δ<sup>13</sup>C (Δδ<sup>13</sup>C) to show the near theoretical kinetic fractionation factor

θ <sub>a</sub>	γ	Chamber δ <sup>13</sup> C	Soil δ <sup>13</sup> C	Δδ <sup>13</sup> C
0.10	3	-24.97	-20.67	-4.3
0.20	3	-24.71	-20.34	-4.37
0.25	3	-24.40	-19.96	-4.44
0.39	3	-22.65	-17.96	-4.69
0.35	1	-20.73	-16.06	-4.67
0.35	10	-24.45	-20.02	-4.43

**Table 2.** Summary data from the simulated comparability and reliability scenarios. Methodologies were neither comparable with one another nor reliable across the range of soil conditions simulated. All isotopic signatures are expressed as offsets (‰) from the actual value of  $-25\text{‰}$  with positive numbers meaning the signatures contain more  $^{13}\text{C}$ , total soil production rate ( $\gamma$ ) and soil diffusivity ( $D$ ) have units of  $\mu\text{mol m}^{-3}\text{s}^{-1}$  and  $\times 10^{-6}\text{m}^2\text{s}^{-1}$ , respectively

Name	$\gamma$	$D$	Static	Purged-K	Purged-S	Bertolini	Mora
Spring	0.6	0.4	0.21	4.39	4.15	2.7	6.1
Summer – Wet	3	0.4	0.18	1.30	5.28	0.59	4.7
Summer – Normal	3	1	0.39	2.40	3.28	1.4	5.3
Summer – Dry	3	3	0.92	4.64	2.23	3.55	6.9

### Comparability and reliability scenarios

Here we seek to assess the comparability (how different methods compare with each other under the same soil conditions) and reliability (how a single method varies across soil conditions) of these chamber methods using four hypothetical field scenarios. Simulated field scenarios include a 'Spring' scenario, with wet soils and low respiration rate and three 'Summer' scenarios; (1) Summer – Wet, where soils are wet but respiration rates are high; (2) Summer – Normal, where soils are moist and respiration rates are high; and (3) Summer – Dry, where soils are dry and respiration is high. The specific model parameters used to simulate these scenarios are outlined in Table 2. All the scenario simulations were performed with a 2.5 cm soil collar and analyzed using the protocols presented in the Experimental section.

The resulting  $\delta_r$  estimates produced by each methodology for each scenario are presented in Table 2. These results clearly show that (1) using a single methodology under different field conditions does not produce reliable estimates of the value of  $\delta_r$  and (2) comparison of data collected using different measurement methodologies is impossible because of strong method specific biases in  $\delta_r$  estimates. In some cases the bias caused by changing environmental conditions reached values of 3‰, which, if considered in the context of past  $\delta_r$  studies (i.e. Ekblad and Högberg<sup>5</sup>), is large enough to completely account for  $\delta_r$  variations that were thought to occur due to environmentally induced changes in the  $\delta^{13}\text{C}$  signature of produced  $\text{CO}_2$ .

### RECOMMENDATIONS AND CONCLUSIONS

Each methodology evaluated in this paper was found to be subject to some bias resulting from the perturbation of the steady-state diffusion profile. In all cases the most significant bias arose due to lateral diffusion of soil  $\text{CO}_2$  around the chamber soil collar. We believe that quasi-steady or steady-state methods will eventually offer the most robust estimates of  $\delta_r$ ; however, work still needs to be done to develop a steady-state method that does not bias results. It will also be crucial to couple chamber theory with experimental and field results to ensure that the data gained from current and future studies is sound and unbiased.

In the meantime, for laboratory work where the system of interest can easily be constrained to 1-D (i.e. using closed

wall containers), we recommend using the Bertolini method as it provided an unbiased estimate of  $\delta_r$  under the assumption of 1-D gas transport. It is more difficult to make a sound recommendation for a chamber system to use at field sites. For the field scenarios presented in this paper, simulations of the Keeling plot method offered the most reliable results across the field scenarios considered, with a variation of only 1‰ compared with 1–3‰ for the other methodologies. However, over a wider range of chamber deployment times and diffusive scenarios the error due to Keeling plot non-linearity is shown to be as high as 4‰.<sup>10</sup> Given these significant errors due to non-linearity and potential errors inherent in linear regression and extrapolation procedures,<sup>8,11</sup> we cannot recommend the Keeling plot approach for use in the field, especially for studies that are exploiting small isotopic source differences. Instead we suggest that for chamber time series data that has already been collected according to a Keeling type approach, the model presented here (or other similar 3-D diffusion models) provides a suitable alternative for determining actual source signatures. It requires detailed soil-specific information ( $\text{CO}_2$  production rate and expected depth distribution, atmospheric  $\delta^{13}\text{C}$ - $\text{CO}_2$ , diffusivity, chamber collar insertion depth, etc.) and may be computationally intensive if fitting of unknown parameters is required but it can appropriately account for non-linearity in isotope mixing, eliminating at least one source of bias. Of course, error will still exist in model estimates of  $\delta_r$  because the model is simplified and does not truly simulate field conditions. Researchers must always consider the uncertainty inherent in isotope measurements due to depth-varying isotopic signatures, time-varying root signals, spatial heterogeneity in the soil diffusive environment and possible advective processes (i.e. wind pumping).

Isotopic measurements of ecosystem efflux can provide a wealth of information, which cannot be obtained with measurement of only  $\text{CO}_2$  efflux rates. Because of this, the development of a robust, accurate sampling methodology will be crucial in studying these processes and gaining more information about ecosystem and global scale carbon cycling processes. It is important, however, not to overlook inconsistencies in data and assumptions inherent in these methodologies. To gain the best estimates of  $\delta_r$ , researchers should continually evaluate the theoretical underpinnings of the tools and approaches used to acquire this important data.

## Acknowledgements

This research was funded by the Natural Sciences and Engineering Research Council of Canada through grants to both authors. Thanks to K. E. A. Ohlsson for the use of his experimental data in Fig. 6, to C. Werner for providing us with data on potential soda lime fractionation, and to three anonymous reviewers for their helpful comments and insight.

## REFERENCES

- Ohlsson KEA, Bhupinderpal S, Holm S, Nordgren A, Lövdahl L, Högberg P. *Soil Biol. Biochem.* 2005; **37**: 2273.
- Kayler ZE, Sulzman EW, Marshall JD, Mix A, Rugh WD, Bond BJ. *Rapid Commun. Mass Spectrom.* 2008; **22**: 2533.
- Buchmann N, Ehleringer JR. *Agric. Forest Meteorol.* 1998; **89**: 45.
- Ekblad A, Högberg P. *Plant Soil* 2000; **219**: 197.
- Ekblad A, Högberg P. *Oecologia* 2001; **127**: 305.
- Högberg P, Ekblad A. *Soil Biol. Biochem.* 1996; **28**: 1131.
- Cerling TE, Solomon DK, Quade J, Bowman JR. *Geochim. Cosmochim. Acta* 1991; **55**: 3403.
- Pataki DE, Ehleringer JR, Flanagan LB, Yakir D, Bowling DR, Still CJ, Buchmann N, Kaplan JO, Berry JA. *Global Biogeochem. Cycles* 2003; **17**: 1022. DOI: 10.1029/2001GB00185023.
- Risk D, Kellman L. *Geophys. Res. Lett.* 2008; **35**: L02403.
- Nickerson N, Risk D. *Geophys. Res. Lett.* 2009; **36**: L08401.
- Zobitz JM, Keener JP, Schnyder H, Bowling DR. *Agric. Forest Meteorol.* 2006; **136**: 56.
- Flanagan LB, Brooks JR, Varney GT, Berry SC, Ehleringer JR. *Global Biogeochem. Cycles* 1996; **10**: 629.
- Mora G, Raich JW. *Rapid Commun. Mass Spectrom.* 2007; **21**: 1866.
- Subke J, Inglema I, Peresotti A, Vedove GD, Cotrufo MF. *Soil Biol. Biochem.* 2004; **36**: 1013.
- Bertolini T, Inglema I, Rubino M, Marzaioli F, Lubritto C, Subke J, Peresotti A, Cotrufo MF. *Isot. Environ. Health Stud.* 2006; **42**: 57.
- Midwood AJ, Thornton B, Millard P. *Rapid Commun. Mass Spectrom.* 2008; **22**: 2073.
- Livingston GP, Hutchinson GL, Spartalin K. *Geophys. Res. Lett.* 2005; **32**: L24817.
- Nickerson N, Risk D. *J. Geophys. Res.* 2009; **114**: G01013.
- Pumpanen J, Ilvesniemi H, Hari P. *Soil Sci. Soc. Am. J.* 2003; **67**: 402.
- McCarthy KA, Johnson RL. *J. Environ. Qual.* 1995; **24**: 49.
- Cerling TE. *Earth Planet. Sci. Lett.* 1984; **71**: 229.
- Well R, Flessa H. *Rapid Commun. Mass Spectrom.* 2008; **22**: 2621.
- Amundson R, Stern L, Baisden T, Wang Y. *Geoderma* 1998; **82**: 83.
- Werner C, Hasenbein N, Maia R, Beyschlag W, Máguas C. *Rapid Commun. Mass Spectrom.* 2007; **21**: 1352.